International Journal of Mathematical Archive-8(10), 2017, 131-142
Available online through www.ijma.info ISSN 2229 – 5046

HEAT AND MASS TRANSFER IN RADIATIVE MHD FLUID FLOW OVER A PERMEABLE VERTICAL PLATE IN THE PRESENCE OF THE HEAT SOURCE

K. RAJESHWAR REDDY[1*], M. CHENNA KRISHNA REDDY[2]

**[1]Department of Mathematics,
Malla Reddy College of Eng. & Tech. Medchal-500100,**

**[2]Department of Mathematics,
Osmania University, Hyderabad-500007, Telangana State, India.**

(Received On: 05-09-17; Revised & Accepted On: 02-10-17)

ABSTRACT

Numerical investigation is carried out for analyzing the heat and mass transfer in radiative magneto hydrodynamics fluid flow over a permeable vertical plate in the presence of the heat source. The governing systems of partial differential equations are transformed to dimensionless equations using dimensionless variables. The dimensionless equations are solved numerically by using finite element method. With the help of graphs, the effects of the various important parameters entering into the problem on the dimensionless velocity, dimensionless temperature and dimensionless concentration fields within the boundary layer are discussed. Numerical values of friction factor, local Nusselt and Sherwood numbers are tabulated.

Key words: *Heat and Mass transfer, MHD, Heat source, FEM.*

1. INTRODUCTION

In many transport processes existing in nature and in industrial applications in which heat and mass transfer is a consequence of buoyancy effects caused by diffusion of heat and chemical species, the study of such processes is useful for improving a number of chemical technologies such as polymer production, enhanced oil recovery, underground energy transport, manufacturing of ceramics and food processing. Heat and mass transfer from different geometries embedded in porous media has many engineering and geophysical applications such as drying of porous solids, thermal insulations, and cooling of nuclear reactors. At high operating temperature, radiation effects can be quite significant. Many processes in engineering areas occur at high temperature and knowledge of radiation heat transfer becomes very important for the design of reliable equipment's, nuclear plants, gas turbines and various propulsion devices or aircraft, missiles, satellites and space vehicles.

Ahmed *et al.* [1] analyzed the convective MHD oscillatory flow past a uniformly moving infinite vertical plate taking into account variable suction velocity and heat generation. The effects of Hall current on the fluid flow and heat transfer in rotating channels have many engineering applications inflows of laboratory plasmas, in MHD power generation, in MHD accelerators, and in several astrophysical and geophysical situations. Takhar *et al.* [2] extended the problem with variable suction and heat generation. Deka *et al.* [3] investigated the effect of first order homogeneous chemical reaction on the process of an unsteady flow past an infinite vertical plate with a constant heat and mass transfer. Muthucumaraswamy and Ganesan [4] discussed the effect of the chemical reaction and injection on flow characteristics in an unsteady upward motion of an isothermal plate. MHD flow of a uniformly stretched vertical permeable surface in the presence of heat generation/absorption and a chemical reaction has been considered by Chamkha [5]. Ibrahim *et al.* [6] obtained the analytical solution for unsteady MHD free convection flow past a semi – infinite vertical permeable moving plate with heat source and chemical reaction. Rahman *et al.* [7] studied heat transfer in micro polar fluid with temperature dependent fluid properties along a non – stretching sheet.

***Corresponding Author: K. Rajeshwar Reddy[1*],
[1]Department of Mathematics, Malla Reddy College of Eng. & Tech. Medchal-500100,***

Based on these applications, Cogley *et al.* [8] showed that in the optically thin limit, the fluid does not absorb its own emitted radiation but the fluid does absorb radiation emitted by the boundaries. Satter and Hamid [9] investigated the unsteady free convection interaction with thermal radiation in a boundary layer flow past a vertical porous plate. Vajravelu [10] studied the flow of a steady viscous fluid and heat transfer characteristic in a porous medium by considering different heating processes. Hossain and Takhar [11] have considered the radiation effect on mixed convection boundary layer flow of an optically dense viscous incompressible fluid along a vertical plate with uniform surface temperature. Raptis [12] investigate the steady flow of a viscous fluid through a porous medium bounded by a porous plate subjected to a constant suction velocity by the presence of thermal radiation. Makinde [13] examined the transient free convection interaction with thermal radiation of an absorbing emitting fluid along moving vertical permeable plate. The effect of the chemical reaction and radiation absorption on the unsteady MHD free convection flow past a semi – infinite vertical permeable moving plate with heat source and suction has been studied by Ibrahim *et al.* [14].

Siva Reddy Sheri and Prasanthi Modugula [15] has explained heat and mass transfer effects on unsteady MHD flow over an inclined porous plate embedded in porous medium with Soret-Dufour and chemical Reaction. Anand Rao *et al.* [16] presented radiation effects on an unsteady MHD vertical porous plate in the presence of homogeneous chemical reaction. Sivaiah [17] analyzed MHD flow of a rotating fluid past a vertical porous flat plate in the presence of chemical reaction and radiation. Mukhopadhyay [18] performed an analysis to investigate the effects of thermal radiation on unsteady mixed convection flow and heat transfer over a porous stretching surface in porous medium.

The object of the present work is to study the heat and mass transfer in radiative magneto hydrodynamics fluid flow over a permeable vertical plate in the presence of the heat source. Similarity transformation is used to transform the governing partial differential equations to ordinary differential equations which are then solved numerically by finite element method.

2. MATHEMATICAL FORMULATION

We consider the unsteady flow of an incompressible viscous, radiating hydro magnetic fluid past an infinite porous heated vertical plate with time – dependent suction in an optically thin environment. The physical model and the coordinate system are shown in figure 1.

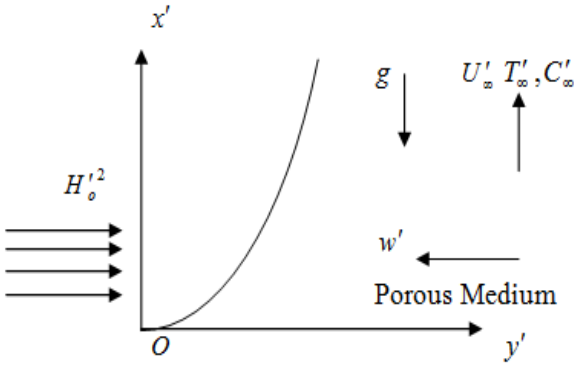

Figure-1: The physical model and coordinate system of the problem

We made the following assumptions:

1. The $x'-$ axis is taken along the vertical infinite porous plate in the upward direction and the $y'-$ axis normal to the plate.
2. At time $t'=0$, the plate is maintained at a temperature T_w', which is high enough to initiate radiative heat transfer.
3. A constant magnetic field $H_0'^2$ is maintained in the y' direction and the plate moves uniformly along the positive $x'-$ direction with velocity U_0.

Under Boussinesq's approximation the flow is governed by the following equations:

Equation of Continuity:

$$\frac{\partial w'}{\partial y'}=0 \tag{1}$$

Momentum Equation:

$$\frac{\partial u'}{\partial t'}+w'\frac{\partial u'}{\partial y'}=\nu\frac{\partial^2 u'}{\partial y'^2}+\frac{\partial U'}{\partial t'}-\left(\frac{\mu^2\sigma_C H_0'^2}{\rho}+\frac{\nu}{k}\right)\left(u'-U'\right)+g\beta\left(T'-T_\infty'\right)+g\beta^*\left(C'-C_\infty'\right) \quad (2)$$

Energy Equation:

$$\frac{\partial T'}{\partial t'}+w'\frac{\partial T'}{\partial y'}=\frac{k}{\rho\, c_P}\left(\frac{\partial^2 T'}{\partial y'^2}-\nabla q_{z'}'\right)-\frac{Q_o}{\rho c_P}(T'-T_\infty') \quad (3)$$

$$\frac{\partial^2 q_{z'}'}{\partial y'^2}-3\alpha^2 q_{z'}'-16\alpha\,\sigma\,T_\infty^{\,3}\frac{\partial T'}{\partial y'}=0 \quad (4)$$

Species Diffusion Equation:

$$\frac{\partial C'}{\partial t'}+w'\frac{\partial C'}{\partial y'}=D\frac{\partial^2 C'}{\partial y'^2} \quad (5)$$

The boundary conditions are

$$\left.\begin{aligned}&u'=0,\ T'=T_w',\ C'=C_w'\ \ on\ \ y'=0\\&u'=U'(t')=w_0'\left(1+\varepsilon\, e^{i\omega' t'}\right),\ T'=T_\infty',\ C'=C_\infty'\ as\ y'\to\infty\end{aligned}\right\} \quad (6)$$

Since the medium is optically thin with relatively low density and $\alpha<<1$ the radiative heat flux given by equation (4) in the spirit of Cogley *et al.* [8] becomes

$$\frac{\partial q_{z'}'}{\partial y'}=4\alpha^2\left(T'-T_\infty'\right) \quad (7)$$

Where $\alpha^2=\int_0^\infty \delta\lambda\frac{\partial B}{\partial T'}$ (8)

Here λ is a frequency.

Further, from equation (1) it is clear that w' is a constant or a function of time only and so we assume

$$w'=-w_0'\left(1+\varepsilon A e^{i\omega' t'}\right) \quad (9)$$

Such that $\varepsilon A<<1$, and the negative sign indicates that the suction velocity is towards the plate.

In view of equations (4), (8) and (9) equations (2), (3) and (5) become

$$\frac{1}{4}\frac{\partial u}{\partial t}-\left(1+\varepsilon A\, e^{i\omega t}\right)\frac{\partial u}{\partial y}=\frac{1}{4}\frac{\partial U}{\partial t}+\frac{\partial^2 u}{\partial y^2}-(M^2)(u-U)+Gr\theta+GcC \quad (10)$$

$$\frac{1}{4}(\Pr)\frac{\partial\theta}{\partial t}-(\Pr)\left(1+\varepsilon A\, e^{i\omega t}\right)\frac{\partial\theta}{\partial y}=\left(\frac{\partial^2}{\partial y^2}-R^2\right)\theta-(\Pr)(S)\theta \quad (11)$$

$$\frac{1}{4}(Sc)\frac{\partial C}{\partial t}-(Sc)\left(1+\varepsilon A\, e^{i\omega t}\right)\frac{\partial C}{\partial y}=\frac{\partial^2 C}{\partial y^2} \quad (12)$$

Where we have used the following dimensionless variables

$$\left.\begin{aligned}&t=\frac{w_0'^2 t'}{4\nu},\ y=\frac{w_0' y'}{\nu},\ u=\frac{u'}{U_0},\ w=\frac{4\nu\omega'}{w_0'^2},\ U=\frac{U'}{U_0},\ \theta=\frac{T'-T_\infty'}{T_w'-T_\infty'}\\&\Pr=\frac{\mu\, c_p}{k},\ Gr=\frac{g\beta\,\nu\left(T_w'-T_\infty'\right)}{U_0 w_0'^2},\ Gc=\frac{g\beta^*\,\nu\left(C_w'-C_\infty'\right)}{U_0 w_0'^2},\ R^2=\frac{4\alpha^2}{\rho\, c_P k w_0'^2}(T_w'-T_\infty'),\\&S=\frac{\nu Q_o}{\rho c_p w_0'^2},\ M^2=\frac{\mu^2\sigma_C H_0'^2}{\rho w_0'^2},\ Sc=\frac{w_o}{D},\ C=\frac{\left(C'-C_\infty'\right)}{\left(C_w'-C_\infty'\right)}\end{aligned}\right\} \quad (13)$$

Equations (10), (11) and (12) are now subject to the boundary conditions

$$\left.\begin{array}{l} u = 0,\quad \theta = 1,\ C = 1 \ \ on \ \ y = 0 \\ u \to 1 + \varepsilon\, e^{i\omega t}\ ,\ \theta \to 0,\ C \to 0 \ \ as \ \ y \to \infty \end{array}\right\} \tag{14}$$

The skin friction, Nusselt number and Sherwood number are important physical parameters for this type of boundary layer flow. The Skin – friction at the plate, which in the non – dimensional form is given by

$$\tau = \frac{\tau'_w}{\rho U_o \nu} = \left(\frac{\partial u}{\partial y}\right)_{y=0} \tag{15}$$

The rate of heat transfer coefficient, which in the non – dimensional form in terms of the Nusselt number is given by

$$Nu = -x\frac{\left(\frac{\partial T'}{\partial y'}\right)_{y'=0}}{T'_w - T'_\infty} \Rightarrow Nu\,\mathrm{Re}_x^{-1} = -\left(\frac{\partial \theta}{\partial y}\right)_{y=0} \tag{16}$$

The rate of mass transfer coefficient, which in the non – dimensional form in terms of the Sherwood number, is given by

$$Sh = -x\frac{\left(\frac{\partial C'}{\partial y'}\right)_{y'=0}}{C'_w - C'_\infty} \Rightarrow Sh\,\mathrm{Re}_x^{-1} = -\left(\frac{\partial C}{\partial y}\right)_{y=0} \tag{17}$$

Where $\mathrm{Re} = \dfrac{U_o x}{\nu}$ is the local Reynolds number.

The mathematical statement of the problem is now complete and embodies the solution of equations (10), (11) and (12) subject to boundary conditions (14).

3. METHOD OF SOLUTION

By applying Galerkin finite element method (Bathe [19] and Reddy [20]) for equation (10) over the element (e), $(y_j \le y \le y_k)$ is:

$$\int_{y_j}^{y_k} \left\{ N^{(e)^T} \left[4\frac{\partial^2 u^{(e)}}{\partial y^2} - \frac{\partial u^{(e)}}{\partial t} + 4B\frac{\partial u^{(e)}}{\partial y} - Du^{(e)} + P \right] \right\} dy = 0 \tag{18}$$

Where $P = \dfrac{\partial U}{\partial t} + 4(Gr)\theta + 4(Gc)C + DU$, $B = 1 + \varepsilon A e^{i\omega t}$, $D = 4(M^2 + \chi^2)$;

Integrating the first term in equation (18) by parts one obtains

$$4N^{(e)^T}\left\{\frac{\partial u^{(e)}}{\partial y}\right\}_{y_j}^{y_k} - \int_{y_j}^{y_k}\left\{ 4\frac{\partial N^{(e)^T}}{\partial y}\frac{\partial u^{(e)}}{\partial y} + N^{(e)^T}\left(\frac{\partial u^{(e)}}{\partial t} - 4B\frac{\partial u^{(e)}}{\partial y} + Du^{(e)} - P \right)\right\} dy = 0 \tag{19}$$

Neglecting the first term in equation (19), one gets:

$$\int_{y_j}^{y_k}\left\{ 4\frac{\partial N^{(e)^T}}{\partial y}\frac{\partial u^{(e)}}{\partial y} + N^{(e)^T}\left(\frac{\partial u^{(e)}}{\partial t} - 4B\frac{\partial u^{(e)}}{\partial y} + Du^{(e)} - P \right)\right\} dy = 0$$

Let $u^{(e)} = N^{(e)}\phi^{(e)}$ be the linear piecewise approximation solution over the element (e) $(y_j \le y \le y_k)$ where $N^{(e)} = \begin{bmatrix} N_j & N_k \end{bmatrix}$, $\phi^{(e)} = \begin{bmatrix} u_j & u_k \end{bmatrix}^T$ and $N_j = \dfrac{y_k - y}{y_k - y_j}$, $N_k = \dfrac{y - y_j}{y_k - y_j}$ are the basis functions. One obtains:

$$4\int_{y_j}^{y_k}\left\{\begin{bmatrix} N_j' N_j' & N_j' N_k' \\ N_j' N_k' & N_k' N_k' \end{bmatrix}\begin{bmatrix} u_j \\ u_k \end{bmatrix}\right\}dy+\int_{y_j}^{y_k}\left\{\begin{bmatrix} N_j N_j & N_j N_k \\ N_j N_k & N_k N_k \end{bmatrix}\begin{bmatrix} \dot{u}_j \\ \dot{u}_k \end{bmatrix}\right\}dy-4B\int_{y_j}^{y_k}\left\{\begin{bmatrix} N_j N_j' & N_j N_k' \\ N_j' N_k & N_k' N_k \end{bmatrix}\begin{bmatrix} u_j \\ u_k \end{bmatrix}\right\}dy$$

$$+D\int_{y_j}^{y_k}\left\{\begin{bmatrix} N_j N_j & N_j N_k \\ N_j N_k & N_k N_k \end{bmatrix}\begin{bmatrix} u_j \\ u_k \end{bmatrix}\right\}dy=P\int_{y_j}^{y_k}\begin{bmatrix} N_j \\ N_k \end{bmatrix}dy$$

Simplifying we get

$$\frac{4}{l^{(e)^2}}\begin{bmatrix} 1 & -1 \\ -1 & 1 \end{bmatrix}\begin{bmatrix} u_j \\ u_k \end{bmatrix}+\frac{1}{6}\begin{bmatrix} 2 & 1 \\ 1 & 2 \end{bmatrix}\begin{bmatrix} \dot{u}_j \\ \dot{u}_k \end{bmatrix}-\frac{4B}{2l^{(e)}}\begin{bmatrix} -1 & 1 \\ -1 & 1 \end{bmatrix}\begin{bmatrix} u_j \\ u_k \end{bmatrix}+\frac{D}{6}\begin{bmatrix} 2 & 1 \\ 1 & 2 \end{bmatrix}\begin{bmatrix} u_j \\ u_k \end{bmatrix}=\frac{P}{2}\begin{bmatrix} 1 \\ 1 \end{bmatrix}$$

Where prime and dot are denotes differentiation w.r.t y and time t respectively. Assembling the element equations for two consecutive elements $(y_{i-1} \le y \le y_i)$ and $(y_i \le y \le y_{i+1})$ following is obtained:

$$\frac{4}{l^{(e)^2}}\begin{bmatrix} 1 & -1 & 0 \\ -1 & 2 & -1 \\ 0 & -1 & 1 \end{bmatrix}\begin{bmatrix} u_{i-1} \\ u_i \\ u_{i+1} \end{bmatrix}+\frac{1}{6}\begin{bmatrix} 2 & 1 & 0 \\ 1 & 4 & 1 \\ 0 & 1 & 2 \end{bmatrix}\begin{bmatrix} \dot{u}_{i-1} \\ \dot{u}_i \\ \dot{u}_{i+1} \end{bmatrix}-\frac{4B}{2l^{(e)}}\begin{bmatrix} -1 & 1 & 0 \\ -1 & 0 & 1 \\ 0 & -1 & 1 \end{bmatrix}\begin{bmatrix} u_{i-1} \\ u_i \\ u_{i+1} \end{bmatrix} \quad (20)$$

$$+\frac{D}{6}\begin{bmatrix} 2 & 1 & 0 \\ 1 & 4 & 1 \\ 0 & 1 & 2 \end{bmatrix}\begin{bmatrix} u_{i-1} \\ u_i \\ u_{i+1} \end{bmatrix}=\frac{P}{2}\begin{bmatrix} 1 \\ 2 \\ 1 \end{bmatrix}$$

Now put row corresponding to the node i to zero, from equation (20) the difference schemes with $l^{(e)} = h$ is:

$$\frac{4}{h^2}\left[-u_{i-1}+2u_i-u_{i+1}\right]+\frac{1}{6}\left[\dot{u}_{i-1}+4\dot{u}_i+\dot{u}_{i+1}\right]-\frac{4B}{2h}\left[-u_{i-1}+u_{i+1}\right]+\frac{D}{6}\left[u_{i-1}+4u_i+u_{i+1}\right]=P \quad (21)$$

Applying the trapezoidal rule, following system of equations in Crank – Nicholson method are obtained:

$$A_1u_{i-1}^{n+1}+A_2u_i^{n+1}+A_3u_{i+1}^{n+1}=A_4u_{i-1}^{n}+A_5u_i^{n}+A_6u_{i+1}^{n}+P^* \quad (22)$$

Now from equations (11) and (12) following equations are obtained:

$$B_1\theta_{i-1}^{n+1}+B_2\theta_i^{n+1}+B_3\theta_{i+1}^{n+1}=B_4\theta_{i-1}^{n}+B_5\theta_i^{n}+B_6\theta_{i+1}^{n} \quad (23)$$

$$C_1C_{i-1}^{n+1}+C_2C_i^{n+1}+C_3C_{i+1}^{n+1}=C_4C_{i-1}^{n}+C_5C_i^{n}+C_6C_{i+1}^{n} \quad (24)$$

Where $A_1=2-12Brh-Dk-24r,\ A_2=8+4Dk+48r,\ A_3=2+12Brh+Dk-24r,$

$A_4=2-12Brh-Dk+24r,\ A_5=8-4Dk-48r,\ A_6=2+12Brh+Dk+24r,$

$B_1=2(\mathrm{Pr})-12(\mathrm{Pr})Brh-4R^2k-24r-4(\mathrm{Pr})Sk,\ B_2=8(\mathrm{Pr})+48r+16R^2k+16(\mathrm{Pr})Sk,$

$B_3=2(\mathrm{Pr})+12(\mathrm{Pr})Brh+4R^2k-24r+4(\mathrm{Pr})Sk,$

$B_4=2(\mathrm{Pr})-12(\mathrm{Pr})Brh-4R^2k+24r-4(\mathrm{Pr})Sk,$

$B_5=8(\mathrm{Pr})-48r-16R^2k-16(\mathrm{Pr})Sk,\ B_6=2(\mathrm{Pr})+12(\mathrm{Pr})Brh-4R^2k+24r-4(\mathrm{Pr})Sk,$

$C_1=2(Sc)-12(\mathrm{Pr})Brh-24r,\ C_2=8(Sc)+48r,\ C_3=2(Sc)+12(Sc)Brh-24r,$

$C_4=2(Sc)-12(Sc)Brh+24r,\ C_5=8(Sc)-48r,\ C_6=2(Sc)+12(Sc)Brh+24r,$

$$P^*=12Pk=12k\left(\frac{\partial U}{\partial t}+4(Gr)\theta+DU\right),$$

Here r= $\frac{k}{h^2}$ and h, k are mesh sizes along y – direction and time – direction respectively. Index i refers to space and j refers to the time. In the equations (22), (23) and (24), taking $i = 1(1)n$ and using boundary conditions (14), then the following system of equations are obtained:

$$A_i X_i = B_i \quad i = 1(1)3 \tag{25}$$

where $A_i^{'}$s are matrices of order n and X_i, $B_i^{'}$s are column matrices having n – components. The solutions of above system of equations are obtained by using Thomas algorithm for velocity, temperature and concentration. Also, numerical solutions for these equations are obtained by C – programme. In order to prove the convergence and stability of Galerkin finite element method, the same C – programme was run with smaller values of h and k no significant change was observed in the values of u, θ and C. Hence the Galerkin finite element method is stable and convergent.

4. RESULTS AND DISCUSSIONS

In order to get physical insight into the problem, we have carried out numerical calculations for non-dimensional velocity field, temperature field, species concentration field, skin friction, Nusselt number and Sherwood number at the walls by assigning some specific values to the parameters entering into the problem and the effects of these values on the above fields are demonstrated graphically and tables. The following parameter values are adopted for computations unless otherwise indicated in the figures and table: $Gr = 1.0, Gm = 1.0,\ M = 2.0, K = 1.0, \Pr = 0.71, R = 2.0, S = 1.0,$ $Sc = 0.22, \varepsilon = 0.1, \omega = 0.1, t = 1.0.$ The temperature and the species concentration are coupled to the velocity via Grashof number (Gr) and Modified Grashof number (Gc) as seen in equation (10). For various values of Grashof number and Modified Grashof number, the velocity profiles u are plotted in figures (2) and (3). The Grashof number (Gr) signifies the relative effect of the thermal buoyancy force to the viscous hydrodynamic force in the boundary layer. As expected, it is observed that there is a rise in the velocity due to the enhancement of thermal buoyancy force. Also, as Gr increases, the peak values of the velocity increases rapidly near the porous plate and then decays smoothly to the free stream velocity. The Modified Grashof number (Gc) defines the ratio of the species buoyancy force to the viscous hydrodynamic force. As expected, the fluid velocity increases and the peak value is more distinctive due to increase in the species buoyancy force. The velocity distribution attains a distinctive maximum value in the vicinity of the plate and then decreases properly to approach the free stream value. It is noticed that the velocity increases with increasing values of Modified Grashof number (Gc).

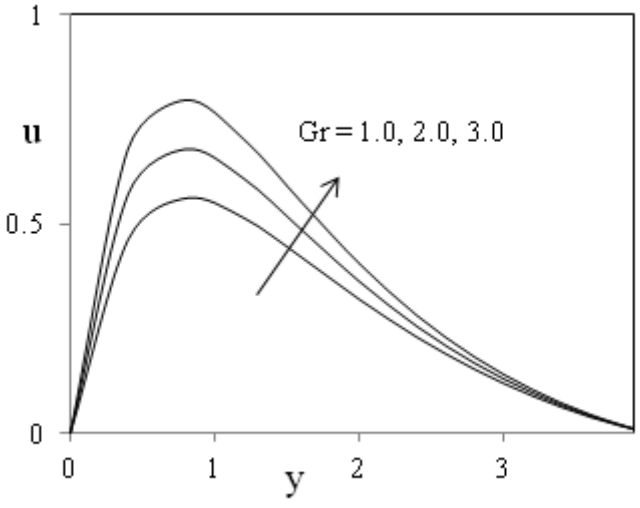

Figure-2: Velocity profiles for different values of thermal Grashof number Gr

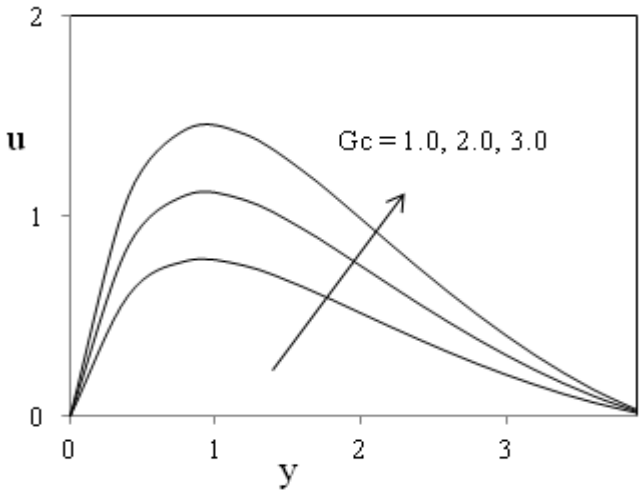

Figure-3: Velocity profiles for different values of solutal Grashof number Gc

Figure (4) illustrate the velocity profiles for different values of Prandtl number Pr . The numerical results show that the effect of increasing values of Prandtl number result in decreasing velocity. The nature of velocity profiles in presence of foreign species such as Hydrogen (Sc = 0.22), Helium (Sc = 0.22), Oxygen (Sc = 0.60) and Water vapour (Sc = 0.66) are shown in figure (5). The flow field suffers a decrease in primary velocity at all points in presence of heavier diffusing species.

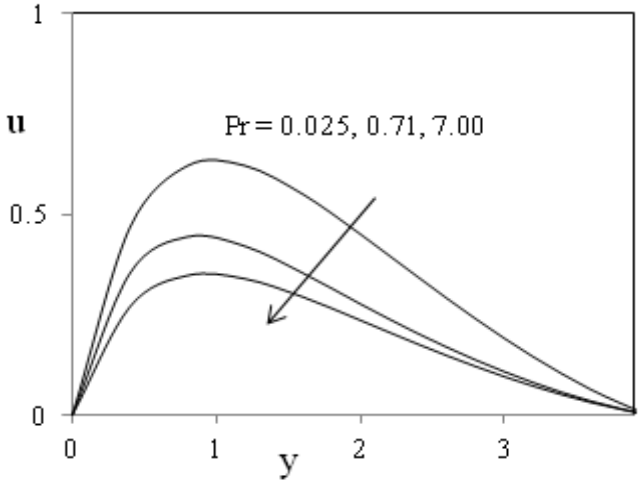

Figure-4: Velocity profiles for different values of Prandtl number Pr

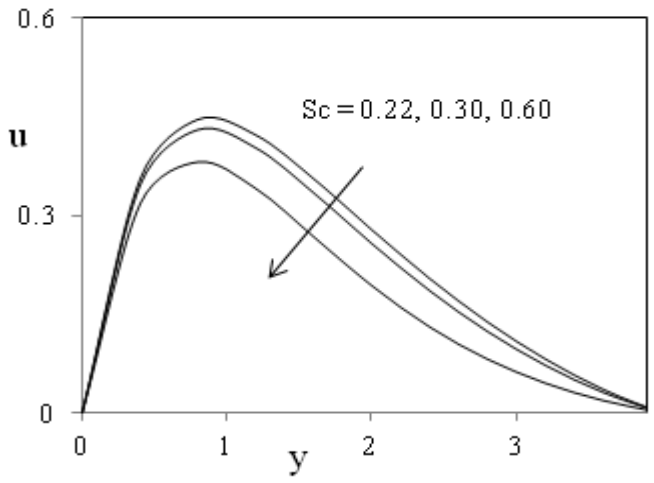

Figure-5: Velocity profiles for different values of Schmidt number Sc

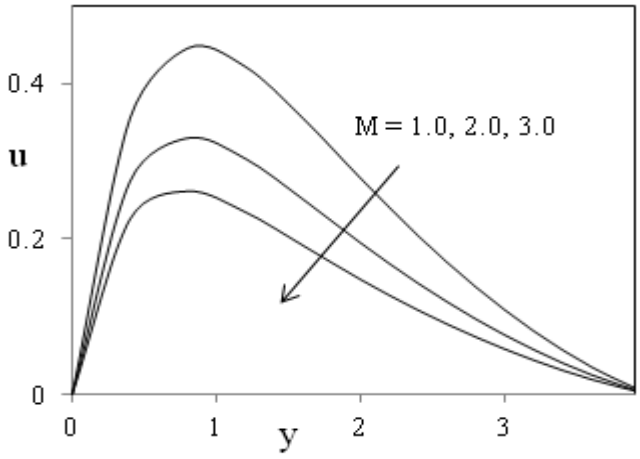

Figure- 6: Velocity profiles for different values of Hartmann number M

The effect of the magnetic field parameter M is shown in figure (6) in case of cooling of the plate. It is observed that the velocity of the fluid decreases with the increase of the magnetic field parameter values. The decrease in the velocity as the Hartmann number M increases is because the presence of a magnetic field in an electrically conducting fluid introduces a force called the Lorentz force, which acts against the flow if the magnetic field is applied in the normal direction, as in the present study. This resistive force slows down the fluid velocity component as shown in figure (6).

The effect of the thermal radiation parameter R on the primary velocity and temperature profiles in the boundary layer are illustrated in figures (7) and (8) respectively. Increasing the thermal radiation parameter R produces significant increase in the thermal condition of the fluid and its thermal boundary layer. This increase in the fluid temperature induces more flow in the boundary layer causing the velocity of the fluid there to increase.Figure (9) and (10) has been plotted to depict the variation of velocity and temperature profiles against y for different values of heat source parameter S by fixing other physical parameters. From this Graph we observe that velocity and temperature decrease with increase in the heat source parameter S because when heat is absorbed, the buoyancy force decreases the temperature profiles.

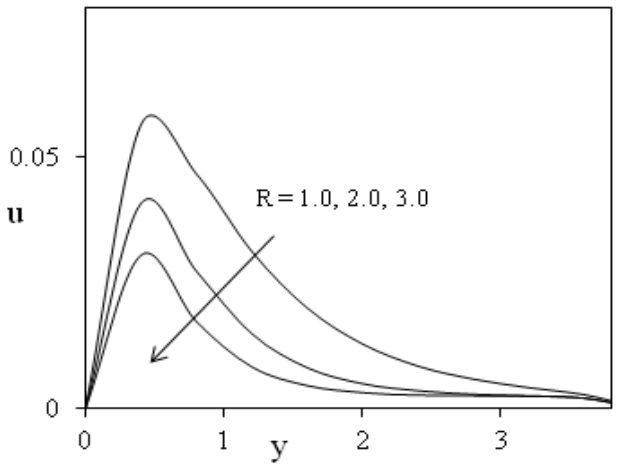

Figure-7: Velocity profiles for different values of Thermal radiation parameter R

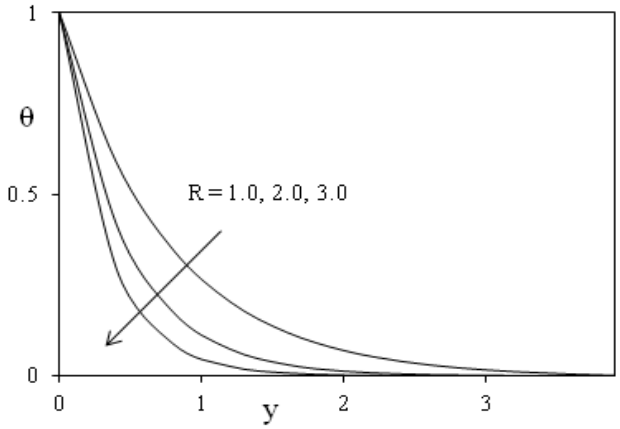

Figure -8: Temperature profiles for different values of Thermal radiation parameter R

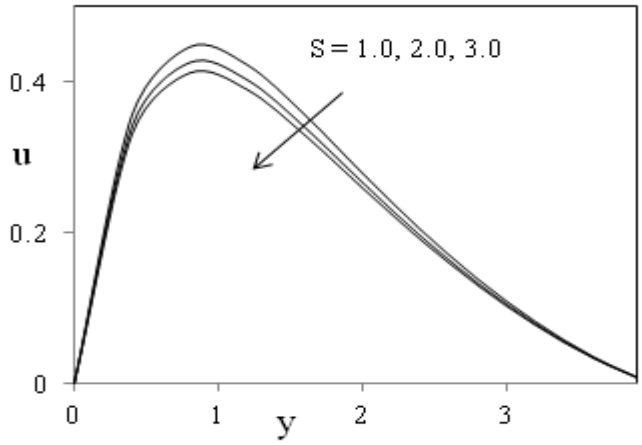

Figure-9: Velocity profiles for different values of Heat source parameter S

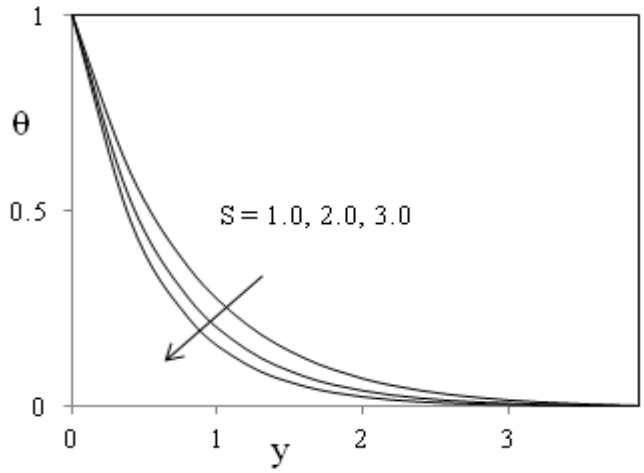

Figure-10: Temperature profiles for different values of Heat source parameter S

Figure (11) illustrate the temperature profiles for different values of Prandtl number $\Pr$. It is observed that the temperature decrease as an increasing the Prandtl number. The reason is that smaller values of Pr are equivalent to increase in the thermal conductivity of the fluid and therefore heat is able to diffuse away from the heated surface more rapidly for higher values of Pr. Hence in the case of smaller Prandtl number the thermal boundary layer is thicker and the rate of heat transfer is reduced.

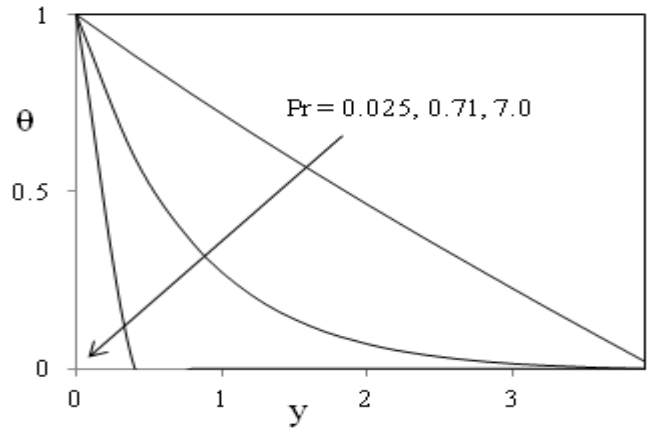

Figure-11: Temperature profiles for different values of Prandtl number Pr

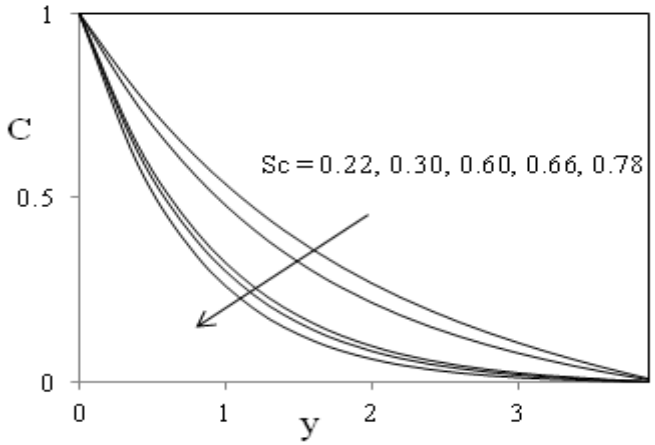

Figure-12: Concentration profiles for different values of Schmidt number Sc

The effects of Schmidt number (Sc) on the concentration field are presented in figures (12). Figure (12) shows the concentration field due to variation in Schmidt number (Sc) for the gasses Hydrogen, Helium, Water – vapour, Oxygen and Ammonia. It is observed that concentration field is steadily for Hydrogen and falls rapidly for Oxygen and Ammonia in comparison to Water – vapour. Thus Hydrogen can be used for maintaining effective concentration field and Water – vapour can be used for maintaining normal concentration field.

Table – 1: Variation of numerical values of Skin – friction (τ) for different values of Gr, Gc, Sc, Pr, M, S and R

Gr	Gc	Pr	Sc	M	S	R	τ
1.0	1.0	0.71	0.22	2.0	1.0	1.0	3.2698
2.0	1.0	0.71	0.22	2.0	1.0	1.0	4.1059
1.0	2.0	0.71	0.22	2.0	1.0	1.0	4.5841
1.0	1.0	7.00	0.22	2.0	1.0	1.0	2.8520
1.0	1.0	0.71	0.60	2.0	1.0	1.0	2.8852
1.0	1.0	0.71	0.22	4.0	1.0	1.0	2.9543
1.0	1.0	0.71	0.22	2.0	2.0	2.0	2.9985
1.0	1.0	0.71	0.22	2.0	1.0	2.0	2.8546

Table – 2: Variation of Nusselt number (Nu) for different values of Pr, S and R

Pr	S	R	Nu
0.71	1.0	1.0	1.9764
7.00	1.0	1.0	1.7530
0.71	2.0	1.0	1.6958
0.71	1.0	2.0	1.8682

Table – 3: Variation of Sherwood number (Sh) for different values of Sc

Sc	Sh
0.22	1.6987
0.30	1.5209
0.60	1.3247

Table – (1) shows the variation of different values Gr, Gc, Pr, Sc, M, S and R on Skin – friction (τ). From this table it is concluded that the Skin – friction (τ) increases as the values of Gr and Gc increase and this behavior is found just reverse with the increase of Pr, Sc, M, S and R. Table – (2) shows the variation of Nusselt number (Nu) different values of Pr, S and R. From this table it is concluded that the Nusselt number (Nu) decreases as the value of Pr, S and R increases. Table – (3) shows the variation of Sherwood number (Sh) different values of Sc. From this table it is observed that Sherwood number (Sh) decreases as the value of Sc increases.

5. CONCLUSIONS

An investigation of the heat and mass transfer in radiative magneto hydrodynamics fluid flow over a permeable vertical plate in the presence of the heat source is affected by the material parameters. The governing equations are approximated to a system of linear partial differential equations by using Galerkin finite element method. The results are presented graphically and we can conclude that the flow field and the quantities of physical interest are significantly influenced by these parameters.

1. The velocity increases as Grashof number Gr, Modified Grashof number Gc, increases. However, the velocity was found to decreases as the Hartmann number M, Prandtl number Pr, Schmidt number Sc, Thermal radiation parameter R, Heat source parameter S are increases.
2. The fluid temperature was found to decreases as the thermal radiation parameter R, heat source parameter S and Prandtl number Pr are increases.
3. The fluid concentration was found to decreases as the Schmidt number Sc increases.

REFERENCES

1. Ahmed, N., and Das, U.N. (1972): Convective MHD oscillatory flow past a uniformly moving infinite vertical plate, *Defence Science Journal* 42, 53–57.
2. Takhar, H.S., Ram, P.C., Singh, S.S. (1992): Hall effects on heat and mass transfer flow with variable suction and heat generation, *Astro. Phys. Space Sci.*191 (1), 101–106.
3. Deka, R., Das, UN., Soundalgekar, VM.(1994): Effects of mass transfer flow past an impulsively started infinite vertical plate with constant heat flux and chemical reaction. Forsch. Ingenieurwes. 60, 284–287.
4. Muthucumaraswamy,R., Ganesan,P.(2001): Effect of the chemical reaction and injection on flow characteristics in an unsteady upward motion of an isothermal plate. J. Appl. Mech. Tech. Phys. 42, 665–671.
5. Chamkha, AJ.(2003): MHD flow of a uniformly stretched vertical permeable surface in the presence of heat generation/absorption and a chemical reaction. Int. Commun. Heat Mass Transfer. 30, 413–422.
6. Ibrahim, FS., Elaiw, AM., Bakr, AA.(2008): Effect of the chemical reaction and radiation absorption on the unsteady MHD free convection flow past a semi-infinite vertical permeable moving plate with heat source and suction. Commun. Nonlinear Sci. Numer. Simul. 13, 1056–1066.
7. Rahman, MM. (2009): Convective flows of micro polar fluids from radiate isothermal porous surfaces with viscous dissipation and Joule heating. Commun. Nonlinear Sci. Numer. Simul. 14, 3018–3030.
8. Cogley, AC., Vincenty, WE., Gilles, SE.(1968): Differential approximation for radiation in a non-gray gas near equilibrium, AIAA J. 6, 551–553.
9. Abdus Sattar,MD., Kalim, MD., Hamid.(1996): Unsteady free – convection interaction with thermal radiation in a boundary layer flow past a vertical porous plate. J. Math. Phys. Sci. 30, 25–37.
10. Vajravelu, K.(1994): Flow and heat transfer in a saturated porous medium. ZAMM. 74, 605–614.
11. Hossain, MA., Takhar, H.S.(1996): Radiation effect on mixed convection along a vertical plate with uniform surface temperature. Heat Mass Transfer. 31, 243–248.
12. Raptis, A.(1998): Radiation and free convection flow through a porous medium. Int. Commun. Heat Mass Transfer. 25, 289–295.
13. Makinde,OD.(2005): Free convection flow with thermal radiation and mass transfer past a moving vertical porous plate. Int. Commun. Heat Mass Transfer. 32, 1411–1419.

14. Ibrahim, FS., Elaiw, AM., Bakr, AA.92008): Effect of the chemical reaction and radiation absorption on unsteady MHD mixed convection flow past a semi-infinite vertical permeable moving plate with heat source and suction. Commun. Nonlinear Sci. Numer. Simul. 13, 1056–1066.
15. Siva Reddy Sheriand Prasanthi Modugula (2017): Heat and mass transfer effects on unsteady MHD flow over an inclined porous plate embedded in porous medium with Soret-Dufour and chemical Reaction. International Journal of Applied and Computational Mathematics. 3,1289-1306.
16. Anand Rao J., S. Sivaiah and Sk. Nuslin. (2012): Radiation effects on an unsteady MHD vertical porous plate in the presence of homogeneous chemical reaction. ARPN Journal of Engineering and Applied Sciences. 7,853-859.
17. Sivaiah, S. (2013): MHD flow of a rotating fluid past a vertical porous flat plate in the presence of chemical reaction and radiation. Journal of Engineering Physics and Thermo physics. 86, 1249–1256.
18. Mukhopadhyay, S. (2009): Effect of thermal radiation on unsteady mixed convection flow and heat transfer over a porous stretching surface in porous medium, International Journal of Heat and Mass Transfer. 52 (13), 3261 – 3265.
19. Bathe, K.J. (1996): Finite Element Procedures. Prentice-Hall. New Jersey.
20. Reddy, J.N. (2006): An Introduction to the Finite Element Method. McGraw-Hill Book Company. New York.

Source of support: Nil, Conflict of interest: None Declared.